P H Y S I C A L   R E V I E W   L E T T E R S

Probing Tiny Motions of Nanomechanical Resonators: Classical or Quantum Mechanical?

L. F. Wei,[1,2] Yu-xi Liu,[1] C. P. Sun,[1,3] and Franco Nori[1,4]

[1]*Frontier Research System, The Institute of Physical and Chemical Research (RIKEN), Wako-shi, Saitama, 351-0198, Japan*
[2]*IQOQI, Department of Physics, Shanghai Jiaotong University, Shanghai 200030, China*
[3]*Institute of Theoretical Physics, The Chinese Academy of Sciences, Beijing, 100080, China*
[4]*Physics Department, MCTP, CSCS, The University of Michigan, Ann Arbor, Michigan 48109-1040, USA*

We propose a spectroscopic approach to probe tiny vibrations of a nanomechanical resonator (NAMR), which may reveal classical or quantum behavior depending on the decoherence-inducing environment. Our proposal is based on the detection of the voltage-fluctuation spectrum in a superconducting transmission line resonator (TLR), which is indirectly coupled to the NAMR via a controllable Josephson qubit acting as a quantum transducer. The classical (quantum mechanical) vibrations of the NAMR induce symmetric (asymmetric) Stark shifts of the qubit levels, which can be measured by the voltage fluctuations in the TLR. Thus, the motion of the NAMR, including if it is quantum mechanical or not, could be probed by detecting the voltage-fluctuation spectrum of the TLR.

Introduction.—Since the beginning of quantum theory, many researchers have tried to monitor macroscopic quantum effects with mechanical resonators (see, e.g., [1]). This relates to the debate on the quantum-classical mechanics boundary for macroscopic objects and the mechanisms of quantum decoherence [2]. Besides superconductivity and Bose-Einstein condensates, quantum oscillations of nanomechanical resonators (NAMRs) could also provide an attractive platform for testing quantum phenomena at macroscopic scales. Also, reaching the quantum limit of mechanical motions could open new avenues of technology [3] in, e.g., high precision measurement, quantum computation, and even gravitational wave detection.

A mechanical resonator may reveal either quantum or classical behavior, depending on the decoherence-inducing environment [2]. Phenomenologically (see, e.g., Ref. [4]), if the energy ($h\nu$) of the vibration (with frequency ν) quanta is larger than the thermal energy $k_B T$, then the mechanical oscillation could be regarded as quantum mechanical. NAMRs with low thermal occupation number have recently been experimentally studied [4,5]. These nanodevices, containing 10^{10}–10^{12} atoms, work at very low temperatures (in the mK range) and sufficiently high frequencies (GHz range), approaching the quantum limit. A formidable challenge (see, e.g., [4,5]) in this field is how to sensitively detect the quivering of the detected nanodevice, and quantitatively verify whether it is quantum mechanical or not. Indeed, it is difficult to directly detect [5,6] the tiny displacements of a NAMR, vibrating at GHz frequencies, using the available displacement-detection techniques. Also, the usual position-measurement method is ultimately limited by the always-present ''zero-point motion'' fluctuations in the quantum regime [1].

Here, we propose a promising indirect method to detect the mechanical oscillation of a NAMR approaching its quantum limit. Instead of attempting to further improve the sensitivity of the usual force-displacement detection [5]

or to redesign the tested nanostructure [4], our proposal is based on the detection of the voltage-fluctuation spectrum in a superconducting transmission line resonator (TLR). A controllable Josephson qubit, acting as a quantum electro-mechanical transducer [7], is used to couple the NAMR to the TLR.

Our approach is conceptually similar to that in quantum optics for verifying the field quantization in a cavity [8], and provides a quantitative test to distinguish the two types of mechanical motions, either quantum or classical. Namely, compared to the spectrum of the TLR without a NAMR, the classical motion of the NAMR only symmetrically increases the vacuum Rabi splitting, while the quantum motion of the NAMR further shifts the positions of the peaks to the right. Physically, this difference originates from the commutativity of the classical variables α and α^*, for classical oscillators, as opposed to the noncommutativity of the corresponding bosonic operators $\hat{b}$ and $\hat{b}^\dagger$ for quantum oscillators. Thus, for large detuning, the classical (quantum) NAMR symmetrically (asymmetrically) shifts the qubit levels. The symmetric shifts enlarge the vacuum Rabi splitting symmetrically, and the additional displacement of the excited level in the asymmetric Stark shifts, induced by the quantum NAMR, further shifts the peaks to the right.

Model.—We consider a simple circuit quantum electrodynamics (CQED) system [9,10] schematically sketched in Fig. 1. A Josephson qubit [11], formed by two Cooper-pair boxes connected via two identical Josephson junctions (with capacitance c_J and Josephson energy ε_J), is capacitively coupled to a TLR (of total capacitance C_t, length L), via a capacitance C_0, and an electrostatically modulated NAMR (of mass m and frequency ω_R), via a capacitance $C_x = C_d(1 + x/d)^{-1}$. The oscillating NAMR (driven, e.g., by an external force pulse) modulates the gap (with displacement x around the equilibrium distance d), and thus the coupling capacitance C_x between the NAMR plate and
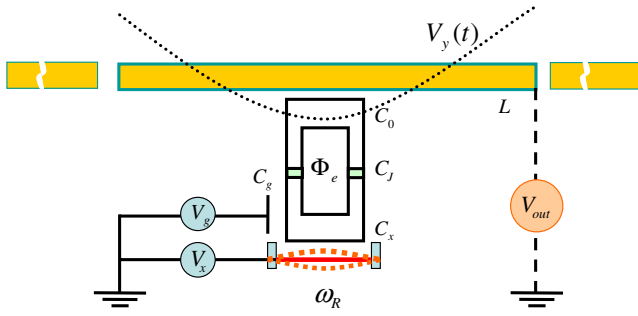
FIG. 1 (color online).   Schematic diagram of a nanomechanical resonator (NAMR) [dashed red (or dark gray) lines, with vibrating frequency ω_R] indirectly coupled to a superconducting transmission line resonator (TLR), shown in yellow (or solid gray), of length L [with voltage distribution $V(y, t) \equiv V_y(t)$ shown by the black dotted line on top] via a Josephson qubit with small junction capacitances. The upper (lower) Cooper-pair box of the qubit capacitively couples to the TLR (NAMR), via a capacitance C_0 (C_x). The voltage-fluctuation spectrum of V_{out}, at the right end of the TLR, reads-out motional information of the NAMR.

the bottom Cooper-pair box. Here, C_d is the gate capacitance between the nonoscillating NAMR plate (corresponding to $x = 0$) and the bottom Cooper-pair box, which is biased by the gate-voltage V_g via the gate capacitance C_g. We assume $C_J = 2c_J \ll C_0 = C_d = C$ to safely neglect the direct interaction between the NAMR and the TLR; their indirect connection is realized by simultaneously coupling to the common qubit, acting as a switchable quantum transducer. The total excess Cooper-pair number n_t in the two boxes (the bottom "b" and upper "u" ones) is $n_t = n_b + n_u = 1$; and $|\downarrow\rangle = |n_b = 1, n_u = 0\rangle$ and $|\uparrow\rangle = |n_b = 0, n_u = 1\rangle$ are the two typical charge states. Near the degenerate point (i.e., $V_x + V_g \approx 0$), this device [11] forms a good two-level artificial "atom," described by the pseudospin operators $\sigma_z = |e\rangle\langle e| - |g\rangle\langle g|$, $\sigma_+ = |e\rangle\langle g|$, and $\sigma_- = |g\rangle\langle e|$, with $|g\rangle = \cos(\alpha/2)|\uparrow\rangle + \sin(\alpha/2)|\downarrow\rangle$ and $|e\rangle = -\sin(\alpha/2)|\uparrow\rangle + \cos(\alpha/2)|\downarrow\rangle$, and $\tan\alpha = E_J/\omega_0$. The "atomic" eigenfrequency $\omega_0 = (E_C^2 + E_J^2)^{1/2}$ could be controlled by the applied gate voltages V_g, V_x, and the biasing external flux Φ_e. In fact, $E_C = eC(V_g + V_x)/(2C_J + C)$ and $E_J = 2\varepsilon_J \cos(\pi\Phi_e/\Phi_0)$, with $\Phi_0 = h/2e$.

Under the usual rotating-wave approximation, the Hamiltonian of our CQED system can be written as

$$H = H_S + \nu\hat{a}^\dagger\hat{a} + \lambda(\sigma_+\hat{a} + \sigma_-\hat{a}^\dagger) + H_{\text{TLR-bath}} + H_{\text{q-bath}},$$

(1)

with $\hbar = 1$. Depending on the different motions of the NAMR, the first term in Eq. (1) takes the different forms: (i) $H_S = \omega_0\sigma_z/2 = H_N$ for the nonoscillation case "N"—when the NAMR plate does not oscillate; (ii) $H_S = H_N + \zeta[\sigma_+ \exp(-i\omega_R t) + \sigma_- \exp(i\omega_R t)] = H_C$ for the classical case "C"—the NAMR plate oscillates classically with frequency ω_R; and (iii) $H_S = H_N + \omega_R\hat{b}^\dagger\hat{b} + \zeta(\sigma_+\hat{b} + \sigma_-\hat{b}^\dagger) = H_Q$ for the quantum case "Q"—the

NAMR plate oscillates quantum mechanically with frequency ω_R, respectively. All higher-order terms of x/d have been neglected [12], as the quivering x of the NAMR is sufficiently small (compared to d), e.g., $x/d \sim 10^{-6}$. The second- and third terms in Eq. (1) describe a selected bare mode with frequency ν in the TLR and its coupling ($\propto \lambda$) to the qubit. The coupling strengths λ and ζ, listed above, are $\lambda = -\sqrt{\nu/C_t}eC \sin\alpha/(2C_J + C)$ and $\zeta = \sqrt{1/(2m\omega_R)}eCV_x \sin\alpha/[2d(2C_J + C)]$, respectively. Dissipation in the NAMR determines [2] the vibrational modes of the NAMR: classical or quantum mechanical, and thus the form of H_S; while dissipation in the selected TLR mode and the Josephson qubit directly influences the voltage fluctuations in the TLR. Here, we describe these two dissipations via the last two terms of Eq. (1): $H_{\text{TLR-bath}} = \sum_j(\omega_j\hat{c}_j^\dagger\hat{c}_j + u_j\hat{c}_j\hat{a}^\dagger + u_j^*\hat{c}_j^\dagger\hat{a})$ and $H_{\text{q-bath}} = \sum_k(\omega_k\hat{d}_k^\dagger\hat{d}_k + v_k\hat{d}_k\sigma_+ + v_k^*\hat{d}_k^\dagger\sigma_-)$, with $\{\hat{c}_j, \hat{c}_j^\dagger, j = 1, 2, 3, \ldots\}$ and $\{\hat{d}_k, \hat{d}_k^\dagger, k = 1, 2, 3, \ldots\}$ being the corresponding bosonic operators of two independent reservoirs: c-bath and d-bath, respectively. Also, u_j (or v_k) is the coupling between the selected TLR mode (or qubit) and the jth (or kth) mode of the c- (or d-) bath.

A central motivation is to detect the motion of the NAMR by measuring the correlation spectrum

$$S_V(\omega) = \frac{1}{2\pi}\int_{-\infty}^{+\infty} d\tau e^{i\omega\tau}\langle\hat{V}(y, t)\hat{V}(y, t + \tau)\rangle_{t\to\infty}$$

$$\propto \int_0^{+\infty} dt_1 \int_0^{+\infty} dt_2 \exp[i\omega(t_2 - t_1)]\langle\hat{a}^\dagger(t_1)\hat{a}(t_2)\rangle$$

(2)

of the voltage $V(y, t)$ at site y [e.g., $V(L, t) = V_{\text{out}}(t)$ in Fig. 1] in the TLR. The second line in Eq. (2) comes from the fact that the voltage $V(y, t)$, contributed by the selected mode of frequency ν along the TLR, is quantized [9]; $\hat{V}(y, t) \propto [\hat{a}^\dagger \exp(-i\nu t) + \hat{a} \exp(i\nu t)]$. We estimate that the voltage signal in the TLR is sufficiently strong, and can be measured by using a standard rf network analyzer [4]. Indeed, the voltage amplitude, even for the fundamental-mode vacuum fluctuation of the typical TLR [10], is up to $V_{\text{rms}} = \sqrt{\nu/C_t} \sim 2 \ \mu\text{V}$, corresponding to an electric field $E_{\text{rms}} \sim 0.2$ V/m, which is much larger than that in the usual optical 3D atom-QED system [8].

Spectra of the TLR.—If the bare TLR (without coupling to the qubit) is excited at a selected mode of frequency ν, the voltage spectrum should have a Lorentzian shape [10,13]: $S_0(\omega) \propto 1/[(\omega - \nu)^2 + (\gamma/2)^2]$, centered at ν and with a width at half height of $\gamma = \nu/Q_\nu$, for the quality factor Q_ν of that mode due to its dissipation.

First, we consider the voltage-fluctuation spectrum $S_N(\omega)$ of the TLR coupled to the qubit, in the absence of NAMR oscillations. In this case $H_S = H_N$, and the system is initially prepared in the state $|\Psi(0)\rangle = |e0_a0_c0_d\rangle$; i.e., the qubit is in its excited state $|e\rangle$ and the field mode and baths are in the vacuum states: $|0_a0_c0_d\rangle = |0_a\rangle \otimes |0_c\rangle \otimes |0_d\rangle$, with $|0_c\rangle = \prod_{j=1}^\infty |0_j\rangle$, $|0_d\rangle = \prod_{k=1}^\infty |0_k\rangle$, respectively.

The wave function of the system at arbitrary time t takes the form [13,14]:

$$|\Psi(t)\rangle = c_1(t)|g1_a0_c0_d\rangle + c_2(t)|e0_a0_c0_d\rangle$$
$$+ \sum_{j=1}^{\infty} C_j(t)|g0_a\{1_j\}0_d\rangle + \sum_{k=1}^{\infty} D_k(t)|g0_a0_c\{1_k\}\rangle,$$

(3)

with $|\{1_j\}\rangle = |1_j\rangle \otimes \prod_{j'\neq j}|0_{j'}\rangle$ and $|\{1_k\}\rangle = |1_k\rangle \otimes \prod_{k'\neq k}|0_{k'}\rangle$. Thus, the measured voltage spectrum is determined by the time-dependence of $c_1(t)$, i.e., $\langle\hat{a}^\dagger(t_1)\hat{a}(t_2)\rangle = c_1^*(t_1)c_1(t_2)$. Without loss of generality and for simplicity, we assume that the qubit is adjusted to resonance with one of the eigenmodes of the TLR [10], e.g., $\omega_0 = \nu = 2\pi \times 6$ GHz. Then, under the usual Weisskopf-Wigner approximation [13], the desirable voltage-fluctuation spectrum can be calculated as $S_N(\omega) \propto \lambda^2|A_+^{-1} - A_-^{-1}|^2/\Delta_N^2$, with $A_\pm = -(\gamma_c + \gamma_d)/4 + i[\omega - (\nu \mp \Delta_N)/2]$, and $\Delta_N = \sqrt{4\lambda^2 + \gamma_c\gamma_d - (\gamma_c + \gamma_d)^2/4}$. This $S_N(\omega)$ is a spectrum with a two-peak structure; each peak has a width at half height of $(\gamma_c + \gamma_d)/2$, and the distance between peaks is the vacuum Rabi splitting Δ_N. Above, γ_c and γ_d are the damping rates of the qubit excited state and the selected TLR mode, respectively.

Second, after preparing the present CQED system (biased by a nonzero gate-voltage V_x) in the initial state $|\Psi(0)\rangle$, we drive the NAMR to oscillate mechanically by a force pulse and then measure the voltage-fluctuation spectrum of the TLR. Usually, the interaction between the NAMR and the qubit works in the large-detuning regime [15]: $\eta = \zeta/\delta \ll 1$, i.e., $\zeta \ll \delta = \omega_0 - \omega_R$. In this limit, the NAMR oscillation does not change the qubit-state populations, and only results in Stark shifts on the qubit levels. Indeed, neglecting higher-order small quantities $O(\eta^2)$, the Hamiltonians H_C and H_Q can be effectively approximated [16] to $H_S^{(C)} = (\omega_0/2 + \zeta^2/\delta)\sigma_z$ and $H_S^{(Q)} = \omega_0\sigma_z/2 + \zeta^2(n_c\sigma_z + |e\rangle\langle e|)/\delta$, respectively. Here, n_c is the quantum occupation number of the quantum-mechanical NAMR. Thus, the tiny motions of the NAMR could be probed, via $S_V(\omega)$, by detecting the NAMR-induced Stark shifts of the qubit levels. Since the NAMR (now oscillating in the large-detuning regime) does not induce any quantum transition in the circuit, the wave function at $t > 0$ of the system with NAMR still has the form of $|\Psi(t)\rangle$ given above. However, the voltage-fluctuation spectrum of the TLR will change to

$$S_C(\omega) \propto \left(\frac{\lambda}{\Delta_C}\right)^2|B_+^{-1} - B_-^{-1}|^2,$$

(4)

with $B_\pm = -(\gamma_c + \gamma_d)/4 \pm \xi_C/2 + i[\omega - (\nu \mp \chi_C)/2]$, $\xi_C = \Delta_C\sin(\theta_C/2)$, $\chi_C = \Delta_C\cos(\theta_C/2)$, for the classical case C; and

$$S_Q(\omega) \propto \left(\frac{\lambda}{\Delta_Q}\right)^2|C_+^{-1} - C_-^{-1}|^2,$$

(5)

with $C_\pm = -(\gamma_c + \gamma_d)/4 \pm \xi_Q/2 + i[\omega - (\nu + \zeta^2/\delta \mp \chi_Q)/2]$, $\xi_Q = \Delta_Q\sin(\theta_Q/2)$, $\chi_Q = \Delta_Q\cos(\theta_Q/2)$, for the quantum case Q, respectively. Above, $\Delta_l = ([4\lambda^2 + \varrho_l^2 + \gamma_c\gamma_d - (\gamma_c + \gamma_d)^2/4]^2 + \rho_l^2(\gamma_c - \gamma_d)^2])^{1/4}$, $\theta_l = \arctan[\rho_l(\gamma_c - \gamma_d)/(4\lambda^2 + \varrho_l^2 + \gamma_c\gamma_d - (\gamma_c + \gamma_d)^2/4)]$, $(l = C, Q)$, and $\varrho_C = 2\zeta^2/\delta$, $\varrho_Q = (2n_c + 1)\zeta^2/\delta$.

In the present strong-coupling CQED system, $2\lambda \gg \gamma_c$, γ_d and $\theta_l \sim 0$, thus, when the NAMR does not oscillate, the two peaks of the measured spectrum $S_N(\omega)$ are approximately at $\omega = \nu/2 \pm \Delta_N/2$ with the vacuum Rabi splitting $\Delta_N \approx 2\lambda$. The classically oscillating NAMR shifts the positions of the two peaks in $S_N(\omega)$ to $\omega \approx (\nu/2 \pm \Delta_C/2)$ and enlarges the vacuum Rabi splitting from Δ_N to Δ_C, with an additional splitting $\Delta_C - \Delta_N \approx \varrho_C^2/(4\lambda) = \zeta^4/(\lambda\delta^2)$. Whereas, if the oscillation of the NAMR is quantum mechanical, not only the vacuum Rabi splitting is enlarged (from Δ_N to Δ_Q) by an increment $\Delta_Q - \Delta_N \approx \varrho_Q^2/(4\lambda) = (n_c + 1/2)^2\zeta^4/(\lambda\delta^2)$, but also the positions of the two peaks are shifted to the right by $\Delta\omega = \zeta^2/(2\delta)$ to $\omega \approx \nu/2 \pm \Delta_Q/2 + \Delta\omega$.

For typical parameters (e.g. [5,10,15], $Q_\nu = 10^4$ for $\nu = \omega_0 = 2\pi \times 6$ GHz, $\omega_R = 2\pi \times 1$ GHz, $C_J/C \sim 0.1$, $\zeta = 2\pi \times 30$ MHz, and $\lambda \sim 2\pi \times 500$ MHz, $\gamma_d = 0.6\gamma_c$), Fig. 2(a) shows the vacuum Rabi splitting of the TLR spectrum $S_N(\omega)$ in the absence of the NAMR. Figure 2(b) shows how the NAMR mechanical oscillations modify the voltage-fluctuation spectrum in the TLR. There, we only show how the left peak of $S_N(\omega)$ is shifted in the presence of the NAMR coupled to the qubit. The shift of the right peak can be analyzed similarly. For the case when there is weak coupling between the possible existing NAMR oscillation and the qubit [e.g., $x/d \sim 1.0 \times 10^{-6}$, yielding $\zeta^2/\delta \sim 200$ kHz in Fig. 2(b)], the effect of increasing the vacuum Rabi splitting is very weak: $\Delta_B - \Delta_N \approx \Delta_C - \Delta_N \sim 80$ Hz, which may not be
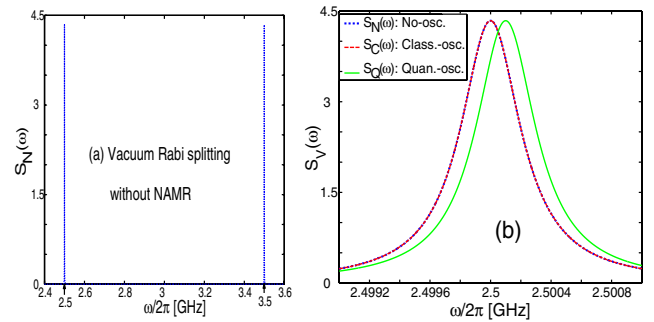

FIG. 2 (color online). Voltage-fluctuation spectra $S_V(\omega)$ of the TLR: (a) vacuum Rabi splitting in the absence of the NAMR vibration; (b) The modifications of the left peak in $S_N(\omega)$ due to the vibrations of the NAMR in the weak coupling case: $\zeta^2/\delta = 200$ kHz. The red (or dark gray) dashed line $S_C(\omega)$ [on top of $S_N(\omega)$] corresponds to the classical NAMR. The green (or gray) solid line $S_Q(\omega)$ (distinguished from $S_N(\omega)$ by a shift to the right) corresponds to the quantum-mechanical NAMR with occupation number $n_c = 1$.
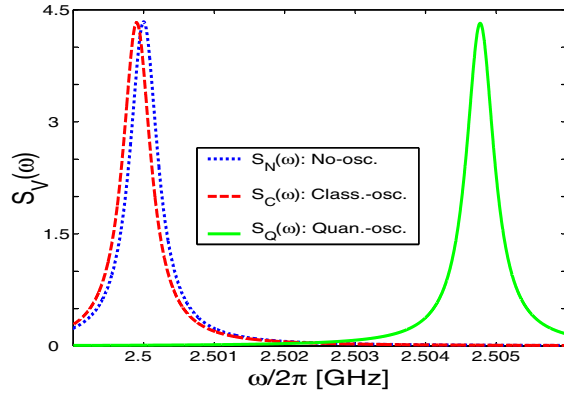
FIG. 3 (color online). Shifts of the left peak of $S_N(\omega)$ [see Fig. 2(a)] when the qubit-NAMR coupling becomes stronger than in the case shown in Fig. 2(b). Here $\zeta^2/\delta = 10$ MHz. In this case, the left peak of $S_N(\omega)$ undergoes a small (large) shift to the left (right) by the classical (quantum mechanical with $n_c = 1$) vibrations of the NAMR.

easily detectable. However, even in such a weak coupling, the effect of shifting the peak of $S_N(\omega)$ to the right, due to the quantum-mechanical NAMR oscillations, should be detectable: $\Delta\omega = \zeta^2/(2\delta) \sim 2\pi \times 100$ kHz.

Given the experimental parameters $\omega_0(= \nu)$, ω_R, and λ, a small decrease of d may yield a large increase in the coupling ζ, and thus the effects discussed above may be much stronger: as $\Delta_l - \Delta_N \propto \zeta^4$ and $\Delta\omega \propto \zeta^2$. Figure 3 shows the modification of $S_N(\omega)$ due to the qubit driven by a strongly coupled NAMR with $x/d \sim 7.1 \times 10^{-6}$, yielding $\zeta^2/\delta \sim 10$ MHz, and thus $\Delta\omega \sim 5$ MHz. In this case, both the classical and quantum-mechanical NAMR can be detected. Compared to the left peak of $S_N(\omega)$, the left peak of $S_C(\omega)$ has been left shifted with a quantity $\chi_C/2 \sim 100$ kHz, just due to the increment χ_C of the vacuum Rabi splitting. While, if the quantum-mechanical NAMR is coupled to the qubit, then the left peak of the spectrum $S_N(\omega)$ will be shifted to the left with $\chi_Q/2$ due to the increased vacuum Rabi splitting χ_Q, and shifted to the right with $\Delta\omega = \zeta^2/2\delta$. The net result is that this peak will be shifted to the right by $\Delta\omega - \chi_Q/2 \approx 2\pi \times 4.8$ MHz, and thus the left peak of $S_Q(\omega)$ would be now centered at $\nu/2 + \Delta\omega - \chi_C/2 \approx 2\pi \times 2504.8$ MHz. This shift could be easily detected.

Conclusion and discussions.—The tiny oscillations of a NAMR should reveal either quantum or classical behavior. We have proposed an effective approach to test this by indirectly probing it. This is because different types of motion of the NAMR would induce different Stark shifts on the qubit levels, and thus modify differently the spectrum of the TLR. Our proposal is experimentally realizable. Also, the mechanical motions of the NAMR in current experiments [5] are approaching the quantum limit, and satisfy the large-detuning condition required in the present proposal. In fact, $\omega_R \lesssim 1$ GHz, $\omega_0 = \nu \sim 6$ GHz in current experiments [5,10], and we estimate $\zeta \sim$

30 MHz (for $C_J/C \sim 0.1$ and $V_x \sim 0.1$ V). This implies that $\eta = \zeta/\delta \sim 6 \times 10^{-3} \ll 1$.

Dissipation exists in the NAMR [17]; i.e., its quality factor Q_R is finite. However, even for the weak NAMR-qubit coupling discussed above (e.g., $\zeta \sim 2\pi \times 30$ MHz), and a relative low quality factor [17], e.g., $Q_R = 10^3$, the decay $\gamma_R = \nu/Q_R$ of the NAMR is still very small: $\gamma_R/\zeta \sim 1/30$. Thus, our proposed test, based on the observation of shifts in the peaks of the voltage spectrum, is not strongly affected by dissipation.

[1] M. F. Bocko and R. Onofrio, Rev. Mod. Phys. **68**, 755 (1996).

[2] See, e.g., A. O. Caldeira and A. J. Leggett, Phys. Rev. A **31**, 1059 (1985); Ann. Phys. (N.Y.) **149**, 374 (1983).

[3] K. C. Schwab and M. L. Roukes, Phys. Today **58**, No. 7, 36 (2005); A. Cho, Science **299**, 36 (2003); M. P. Blencowe, Phys. Rep. **395**, 159 (2004); K. L. Ekinci and M. L. Roukes, Rev. Sci. Instrum. **76**, 061101 (2005).

[4] A. Gaidarzhy *et al.*, Phys. Rev. Lett. **94**, 030402 (2005); **95**, 248902 (2005); K. C. Schwab *et al.*, *ibid.* **95**, 248901 (2005); R. L. Badzey and P. Mohanty, Nature (London) **437**, 995 (2005); W. K. Hensinger *et al.*, Phys. Rev. A **72**, 041405(R) (2005).

[5] See, e.g., M. D. LaHaye *et al.*, Science **304**, 74 (2004); X. M. H. Huang *et al.*, Nature (London) **421**, 496 (2003); R. G. Knobel and A. N. Cleland, Nature (London) **424**, 291 (2003).

[6] N. M. Chtchelkatchev *et al.*, Phys. Rev. B **70**, 193305 (2004); A. A. Clerk *et al.*, *ibid.* **67**, 165324 (2003); A. N. Cleland *et al.*, Appl. Phys. Lett. **81**, 1699 (2002).

[7] M. R. Geller and A. N. Cleland, Phys. Rev. A **71**, 032311 (2005); C. P. Sun *et al.*, Phys. Rev. A **73**, 022318 (2006).

[8] M. Brune *et al.*, Phys. Rev. Lett. **76**, 1800 (1996); J. M. Raimond *et al.*, Rev. Mod. Phys. **73**, 565 (2001).

[9] J. Q. You and F. Nori, Phys. Rev. B **68**, 064509 (2003); A. Blais *et al.*, Phys. Rev. A **69**, 062320 (2004); I. Rau *et al.*, Phys. Rev. B **70**, 054521 (2004).

[10] A. Wallraff *et al.*, Nature (London) **431**, 162 (2004); D. I. Schuster *et al.*, Phys. Rev. Lett. **94**, 123602 (2005).

[11] J. Q. You and F. Nori, Phys. Today **58**, No. 11, 42 (2005); A. Shnirman *et al.*, Phys. Rev. Lett. **79**, 2371 (1997).

[12] P. Zhang *et al.*, Phys. Rev. Lett. **95**, 097204 (2005); I. Martin *et al.*, Phys. Rev. B **69**, 125339 (2004).

[13] M. O. Scully and M. S. Zubairy, *Quantum Optics* (Cambridge University, Cambridge, U.K., 1997).

[14] See, e.g., C. K. Law *et al.*, Phys. Rev. A **52**, 4095 (1995); S. John and T. Quang, Phys. Rev. A **50**, 1764 (1994); X.-H. Wang *et al.*, Phys. Rev. Lett. **88**, 093902 (2002).

[15] A. D. Armour *et al.*, Phys. Rev. Lett. **88**, 148301 (2002); P. Rabl *et al.*, Phys. Rev. B **70**, 205304 (2004); E. K. Irish and K. C. Schwab, Phys. Rev. B **68**, 155311 (2003).

[16] See, e.g., L. F. Wei *et al.*, Phys. Rev. B **71**, 134506 (2005); Y. X. Liu *et al.*, Phys. Rev. A **72**, 033818 (2005).

[17] J. Tamayo, J. Appl. Phys. **97**, 044903 (2005); A. N. Cleland and M. L. Roukes, *ibid.* **92**, 2758 (2002).